

DIVERGENCE AND FLUTTER STABILITY BOUNDARIES OF A ROCKET MODELED AS THIN-WALLED COMPOSITE BEAMS

Melahat Cihan¹
Anadolu University
Eskişehir, Turkey

Seher Eken²
Ondokuz Mayıs University
Samsun, Turkey

Metin Orhan Kaya³
İstanbul Technical University
İstanbul, Turkey

ABSTRACT

In this paper we present the results of the dynamic stability analysis of a flexible spinning aerospace vehicle subjected to thrust load. In order to model the vehicle, we choose a thin-walled composite beam with circular cross-section featuring bending-bending-shear coupled motion. In the presence of gyroscopic forces, we find the divergence and/or the flutter instabilities and plot the stability boundaries of the spinning beam. The solution is provided by the extended Galerkin method (EGM) and the results are plotted to show the effects of ply angle and transverse shear on the dynamic stability of beam. We observe that both ply angle and transverse shear significantly affect the stability behavior of the aerospace vehicle and must be carefully addressed in the design process.

INTRODUCTION

The dynamic stability problem of flexible spinning aerospace vehicles has increasingly attracted attention since early development of space flights. In order to eliminate the instabilities in the design of vehicles, the potential sources have to be clearly identified. One possible cause is the static and/or the dynamic compressive loads acting on these vehicles, which will yield the structure to buckle. For instance, aerospace vehicles may feature dynamic instabilities due to the thrust force acting along their longitudinal axis. This thrust force has a huge impact on vehicle's dynamical characteristics. Besides, the gyroscopic forces, which are generated as soon as the spin starts, may also cause the vehicles to exhibit divergence and flutter instabilities.

The instability problem of aerospace vehicles in flight is generally solved by using a free-free beam subjected to a follower force. Many of studies conducted so far have utilized Euler-Bernoulli and Timoshenko beam theories to establish the model of flexible aerospace

¹ Research Assistant, Email: melahatcihan@anadolu.edu.tr

² Asst. Prof. in Department of Aerospace Engineering, Email: seher.eken@omu.edu.tr

³ Prof. in Department of Aeronautical Engineering, Email: kayam@itu.edu.tr

vehicles. Starting with the work by Beal [Beal, 1965], he studied the stability of a flexible missile under constant and pulsating thrust and the effect of periodically varying thrust perturbations on the stability of the vehicle. Also, Park and Mote [Park and Mote, 1985] inspected the maximum controlled follower force on a free-free beam carrying a concentrated mass. Besides, Platus [Platus, 1992] investigated the aeroelastic stability of slender, spinning missiles and the spin effect on vehicle instability. Lastly, an experimental study on the flutter of visco-elastic cantilevers subjected to a tangential follower force has been conducted by Sugiyama [Sugiyama et al., 1995; Sugiyama et al., 1995]. In his studies, he described the effect of an intermediate concentrated mass on the dynamic stability of cantilevered columns subjected to a rocket thrust and showed comparing with theoretical predictions.

There are also many studies that have solved the problem of dynamical instability of space vehicle using Timoshenko beam theory. For instance, Park [Park, 1987] introduced the influence of rotary inertia and shear deformation parameters on the stability of a free-free beam with a controlled follower force. In another work by Yoon and Kim [Yoon and Kim, 2002], they examined the dynamic stability of a spinning unconstrained beam with a concentrated mass at an arbitrary location and considering pulsating follower force. Abbas et al. [Abbas et al., 2013] also performed transfer matrix method to determine the natural vibration characteristics of realistic thrusting multistage launch vehicle.

Besides Euler, Timoshenko beam theories, in recent years thin-walled beam structures have been widely adopted as primary structural components in aerospace vehicles. Particularly, the applications of these structures in advanced space vehicles has been greatly increased by the advent of fibrous composite materials that provide high strength-to-weight ratios, higher resistance to corrosion and superior fatigue life compared to the traditional materials. In the light of many pioneering and rigorous studies [Song et al., 2001; Song et al., 2002; Song et al., 2000], detailed investigations of thin-walled composite beams have been reported focusing on the vibration and stability of elastically tailored structures.

Thin-walled composite beam theory stands a superior one to establish the model of aerospace vehicles, as it accommodates a number of theoretical issues due to various non-classical effects such as material anisotropy, transverse shear deformation which are inherently present in this kind of structures. Within this context we introduce the thin-walled composite beam with circular cross-section to study the dynamic stability analysis of a flexible spinning aerospace vehicle subjected to thrust force. We mainly aim to find divergence and flutter instabilities and establish the stability boundaries of the spinning beam. For both shearable and unshearable beam models, the eigenvalue problem is solved by the extended Galerkin method (EGM). We present the results addressing the effects of spin speed, axial load, ply angle and transverse shear on the dynamic stability of beam.

FORMULATION

Displacement Field

In this study, we consider the case of a untwisted slender aerospace vehicle having a length of L and its sketch can be found in Figure 1(a). To obtain the dynamical instability characteristics of the aerospace vehicle we use the model of a thin-walled composite beam with a circular cross-section. This beam is fixed at one end, $z=0$ and free at other end, $z=L$. As seen from Figure 1(a), a thrust force acts to the free end of the beam. This thrust force denoted by P is considered to be caused by the rocket motor at the tip of the beam and it is known the compressive axial load. In this case the beam is also spinning along its longitudinal z -axis at a constant rate Ω .

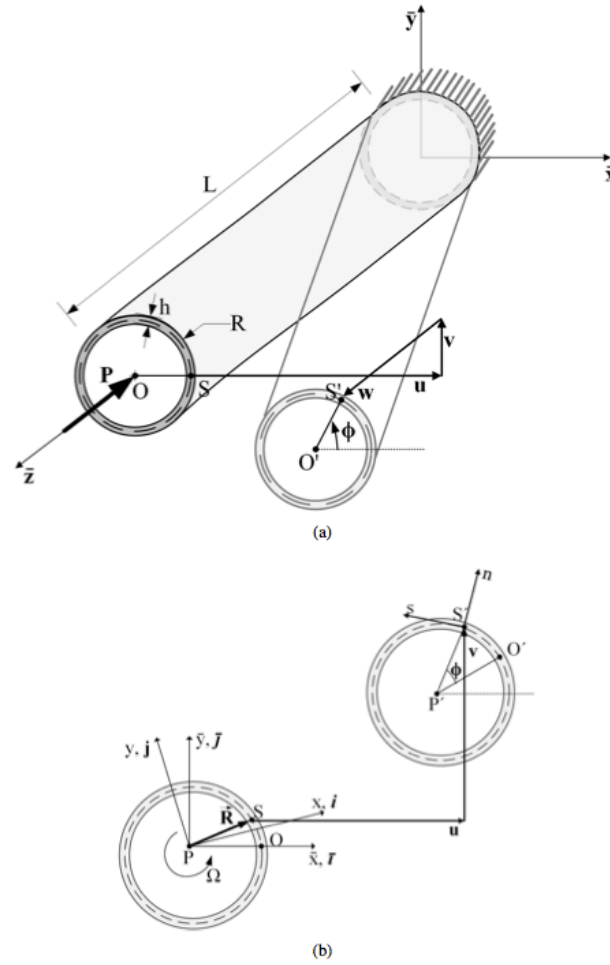


Figure 1: (a) Beam geometry before and after deformation (b) Cross-sectional geometry and kinematic variables

Figure 1(a) also depicts the beam geometry before and after deformation. Point O , which is the pole point, moves to point O' ; while point S , which is located in the mid-cross-section, goes to point S' by the translations u , v and w in x -, y - and z - directions, respectively, and rotates by ϕ . Figure 1(b) also demonstrates the deformation of the middle contour of the cross-section. We lastly adopt a number of kinematic and static assumptions adopted to develop the theory of thin-walled beam with a single-cell cross-section, which can be found in Reference [Eken and Kaya, 2015].

Under these assumptions, the displacement field of a thin-walled beam that undergoes extension, vertical bending, lateral bending and torsion is derived in terms of the translations of pole point:

$$u(x, y, z, t) = u_0(z, t) - y\phi(z, t)$$

$$v(x, y, z, t) = v_0(z, t) - x\phi(z, t)$$

For closed cross-section beams the expression of the axial displacement accounting both for primary and secondary warping is given by [Meitrovich, 1997]

$$w(x, y, z, t) = w_0(z, t) + \left[y - n \frac{dy}{ds} \right] \theta_x(z, t) + \left[x - n \frac{dx}{ds} \right] \theta_y(z, t) - [F_w(s) - nr_t(s)] \phi'(z, t)$$

The position vector of Point S located on the mid-contour which is shown in Figure 1(b):

$$\mathbf{R}(x, y, z, t) = (x + u)\mathbf{i} + (y + v)\mathbf{j} + (z + w)\mathbf{k}$$

Energy expressions

The energy expression of the beam, by using the application of Hamilton's principle is elaborated. For a detailed derivation of the energy expressions for both shearable and unshearable beams, one should refer to Reference [Eken and Kaya, 2015; Qin and Librescu, 2002].

The Governing System of Equations

By the Hamilton's principle, for the thin-walled composite beams featuring CUS configuration, the governing equations of motion are presented in the following [Librescu and Song, 2006]:

$$\delta u_0: \quad a_{34}\theta_x'' + a_{44}(u_0'' + \theta_y') - Pu_0'' = b_1\ddot{u}_0 - 2b_1\Omega\dot{v}_0 - b_1u_0\Omega^2$$

$$\delta v_0: \quad a_{25}\theta_y'' + a_{55}(v_0'' + \theta_x') - Pv_0'' = b_1\ddot{v}_0 - 2b_1\Omega\dot{u}_0 - b_1v_0\Omega^2$$

$$\delta\theta_x: \quad a_{33}\theta_x'' + a_{34}(u_0'' + \theta_y') - a_{55}(v_0' + \theta_x) - a_{25}\theta_y' = (b_4 - b_{14})\ddot{\theta}_x$$

$$\delta\theta_y: \quad a_{22}\theta_y'' + a_{25}(v_0'' + \theta_x') - a_{44}(u_0' + \theta_y) - a_{34}\theta_x' = (b_5 - b_{15})\ddot{\theta}_y$$

with the fixed-free boundary conditions at $z=0$ and $z=L$, respectively:

$$\delta u_0: \quad u_0 = 0 \quad \text{and} \quad a_{34}\theta_x' + a_{44}(u_0' + \theta_y) - Pu_0' = 0$$

$$\delta v_0: \quad v_0 = 0 \quad \text{and} \quad a_{25}\theta_y' + a_{55}(v_0' + \theta_x) - Pv_0' = 0$$

$$\delta\theta_x: \quad \theta_x = 0 \quad \text{and} \quad a_{33}\theta_x' + a_{34}(u_0' + \theta_y) = 0$$

$$\delta\theta_y: \quad \theta_y = 0 \quad \text{and} \quad a_{22}\theta_y' + a_{25}(v_0' + \theta_x) = 0$$

As a special case, unshearable thin-walled beam model is examined and the governing equations of motion are presented in the following:

$$\delta u_0: \quad a_{22}u_0'''' + Pu_0'' + b_1\ddot{u}_0 - (b_5 + b_{15})\ddot{u}_0'' - 2b_1\Omega\dot{v}_0 - b_1u_0\Omega^2 = 0$$

$$\delta v_0: \quad a_{33}v_0'''' + Pv_0'' + b_1\ddot{v}_0 - (b_4 + b_{14})\ddot{v}_0'' + 2b_1\Omega\dot{u}_0 - b_1v_0\Omega^2 = 0$$

with the fixed-free boundary conditions at $z=0$ and $z=L$, respectively:

$$\delta u_0: \quad u_0 = 0 \quad \text{and} \quad a_{22}u_0'''' + Pu_0' - (b_5 + b_{15})\ddot{u}_0' = 0$$

$$\delta v: \quad v_0 = 0 \quad \text{and} \quad a_{33}v_0'''' + Pv_0' - (b_4 + b_{14})\ddot{v}_0' = 0$$

$$\delta u_0': \quad u_0' = 0 \quad \text{and} \quad a_{22}u_0'' = 0$$

$$\delta v_0': \quad v_0' = 0 \quad \text{and} \quad a_{33}v_0'' = 0$$

Solution Methodology

As explained previously, the governing system of equations as well as the pertinent boundary conditions involve the elastic couplings of vertical bending-torsion-(lateral) transverse shear. Obtaining exact solution to these equations is very challenging, besides static boundary conditions are quite complicated. Due to these challenges, the extended Galerkin method, which is based on selecting the weighting functions only by fulfilling the geometric boundary conditions, is used to solve the eigenvalue problem [Librescu and Song, 2006]. This method is proven to be a very powerful tool to obtain accurate and convergent results [Eken and Kaya, 2015].

Initially, the equations of motion are discretized in terms of the following displacements u_0 , v_0 , θ_x and θ_y which are assumed as [Qin and Librescu, 2002]:

$$u_0(z, t) = N_u^T(z) q_u(t)$$

$$v_0(z, t) = N_v^T(z) q_v(t)$$

$$\theta_x(z, t) = N_x^T(z) q_x(t)$$

$$\theta_y(z, t) = N_y^T(z) q_y(t)$$

Here, the trial functions are represented by N_u , N_v , N_x and N_y , which are also called shape functions with the dimension $N \times 1$, while q_u , q_v , q_x and q_y are the vectors of the generalized coordinates. The shape functions used for shearable beams are expressed in following polynomial form:

$$N_u^T(z) = [z \quad z^2 \quad \dots \quad z^N]$$

$$N_v^T(z) = [z \quad z^2 \quad \dots \quad z^N]$$

$$N_x^T(z) = [z \quad z^2 \quad \dots \quad z^N]$$

$$N_y^T(z) = [z \quad z^2 \quad \dots \quad z^N]$$

For unshearable beams the shape function of the bending displacement is different than in shearable counterpart, which is given as:

$$N_u^T(z) = [z^2 \quad z^3 \quad \dots \quad z^{N+1}]$$

$$N_v^T(z) = [z^2 \quad z^3 \quad \dots \quad z^{N+1}]$$

Inserting u_0 , v , θ_x , θ_y into the governing equations of motion, multiplying with the pertinent shape functions (trial functions) and integrating along the spanwise coordinate, we have the free vibration problem as follows:

$$\mathbf{M}\ddot{\mathbf{q}}(t) + \mathbf{C}\dot{\mathbf{q}}(t) + \mathbf{K}\mathbf{q}(t) = 0$$

Here, $[\mathbf{M}]$, $[\mathbf{C}]$ and $[\mathbf{K}]$ represent the mass, damping and the stiffness matrices. In order to solve this system, we represent above equation in state-space form as $\dot{\mathbf{X}}(t) = \mathbf{A}\mathbf{X}(t)$. Here, $\mathbf{X} = [\mathbf{q}^T \quad \dot{\mathbf{q}}^T]^T$ and

$$\mathbf{A} = \begin{bmatrix} \mathbf{0} & \mathbf{I} \\ -\mathbf{M}^{-1}\mathbf{K} & -\mathbf{M}^{-1}\mathbf{C} \end{bmatrix}$$

Assuming $\mathbf{X}(t)$ in the form of $\mathbf{X}(t) = \mathbf{X}e^{(\lambda t)}$, the solution of $\dot{\mathbf{X}}(t) = \mathbf{A}\mathbf{X}(t)$ is solved for eigenvalues λ_j and eigenvectors \mathbf{X}_j ,

$$(\lambda \mathbf{I} - \mathbf{A})\mathbf{X} = 0$$

RESULT AND DISCUSSION

In this section we present the results of dynamic stability analysis of a slender aerospace vehicle modeled as a thin walled composite beam. For the numerical simulations we chose the beam with circular cross-section whose material and geometrical properties can be found in Table 1 [Song et al., 2001]. The influences of the axial load, spin speed, ply angle and transverse shear on the dynamical characteristics of the beam are investigated and numerous results regarding these effects are concluded.

The non-zero stiffness coefficients considered in CUS lay-up are a_{22} , a_{33} , a_{44} , a_{55} , a_{25} and a_{34} which represent the stiffness's of horizontal bending, vertical bending, horizontal transverse shear, vertical transverse shear, horizontal bending-transverse shear coupling and vertical bending-transverse shear coupling, respectively. In order to assess of the dynamical behavior of the thin-walled beam with this configuration, these elastic coefficients are plotted

with respect to ply-angle in Figure 2. Clearly from this figure, due to the circular cross-section we first see that a_{22} perfectly overlaps with a_{33} , and also a_{44} with a_{55} . Secondly, the curve of a_{25} is symmetrical to a_{34} along $\theta = 90^\circ$.

Table 1: Material and geometrical properties of the rocket

Material Properties	
E_{11}	206.8 GPa
$E_{22} = E_{33}$	5.17 GPa
G_{12}	3.10 GPa
$G_{13} = G_{23}$	2.55 GPa
$\nu_{12} = \nu_{31}$	0.00625
ν_{32}	0.25
Density, ρ	1528 kg/m ³
Geometrical Properties	
Radius, R (m)	0.127
Total thickness, h (m)	0.01016
Length, L (m)	2.023
Number of layers, N	6
Lay-ups	$[\theta]_N$

Moreover, the curves of a_{22} and a_{33} with respect to ply-angle reach a peak value at $\theta = 90^\circ$, while a_{44} and a_{55} have their local maximums at $\theta \approx 75^\circ$ and at $\theta \approx 105^\circ$. We lastly observe that the most dominant stiffness coefficients are computed as a_{44} and a_{55} , while a_{22} and a_{33} are the least dominant coefficients compared with others.

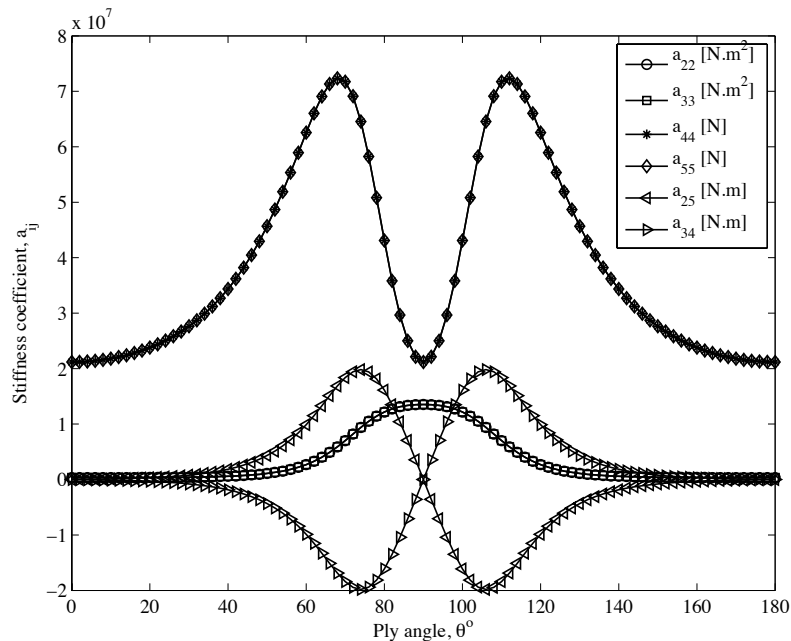


Figure 2: The variation of the stiffness quantities with respect to ply-angle

In this part of results we come to specify the boundaries of divergence and flutter instabilities. This analysis that shows the Ω - P plane for selected ply angles, $\theta = 0^\circ, 30^\circ, 60^\circ, 90^\circ$ in Figures 3-6. In Figure 3, for ply angle $\theta = 0^\circ$, the boundaries/regions are marked with D , F and S denoting the divergence boundary, flutter region and stability region, respectively, and yet we note that in the absence of both axial load and spin speed, the system is defined as stable. The region on the right side of black curve represents the flutter instability F , while the left represents the flutter stable region FS . The divergence instability occurs only on the gray curve, in other words there is no region of divergence instability, and the bottom region of this curve shows the divergent stable region DS .

As we carefully inspect Figures 3-6, we have obtained numerous important results regarding the instability boundaries. First of all, we have observed that stability regions of both regarding flutter and divergence instabilities expand with the increase of ply angle. Secondly, we see that the black lines that represent flutter stable/unstable regions form nearly straight line for higher ply angles, whereas for lower ply angles these lines take a relatively curved form. Lastly and importantly, we see that the transverse shear has a profound effect on the regions of divergence and flutter instabilities. For ply angles $\theta \geq 45^\circ$ the boundary of divergence instability expands, while for ply angles $\theta \leq 45^\circ$, transverse shear has an insignificant effect on the divergence boundary. Nevertheless, the boundary of flutter instability moves forward for ply angles $\theta \leq 30^\circ$, as we observe a slight difference of the results with the inclusion of transverse shear for ply angles $\theta \geq 30^\circ$. We lastly conclude that for both divergence and flutter stability regions the deviation of the results of the shearable theory from the unshearable theory becomes very large at ply angle of $\theta = 60^\circ$.

We further calculate the divergence and flutter instabilities for selected spin speeds and ply angles. P_{div} and $P_{flutter}$ values are computed for both shearable and unshearable beams and tabulated in Table 2. This table also shows a comparison of the instabilities with a previous study of Reference [Song et al., 2002] [*]. As seen, for various spin speeds and ply angle configurations, there is an excellent agreement between the present and published results.

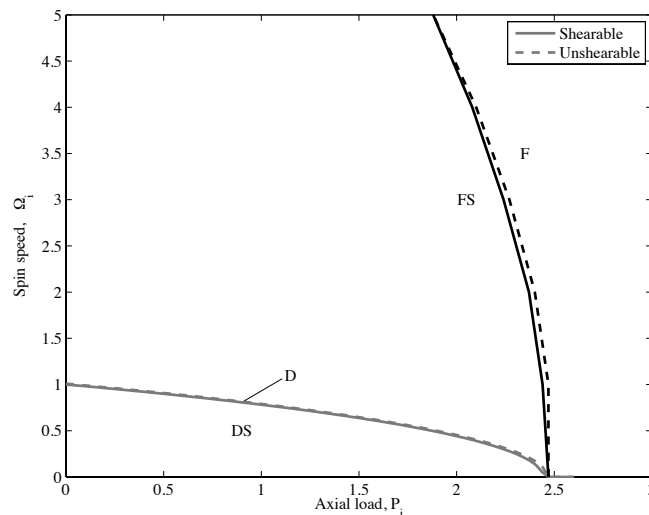


Figure 3: Divergence and flutter instability boundaries in P- Ω plane for $\theta=0^\circ$

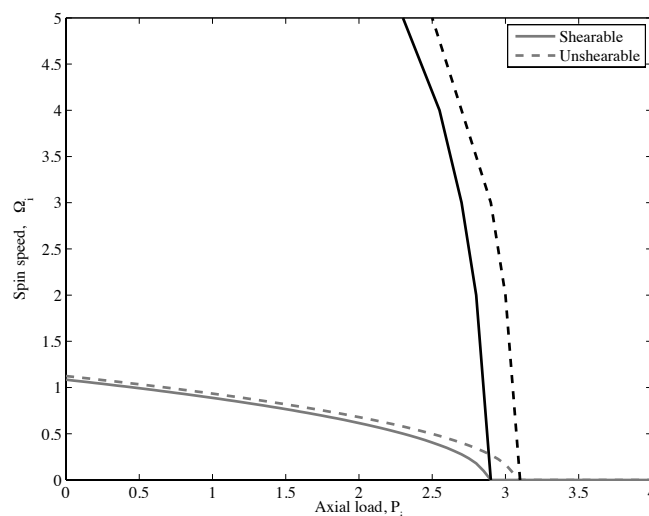


Figure 4: Divergence and flutter instability boundaries in P- Ω plane for $\theta=30^\circ$

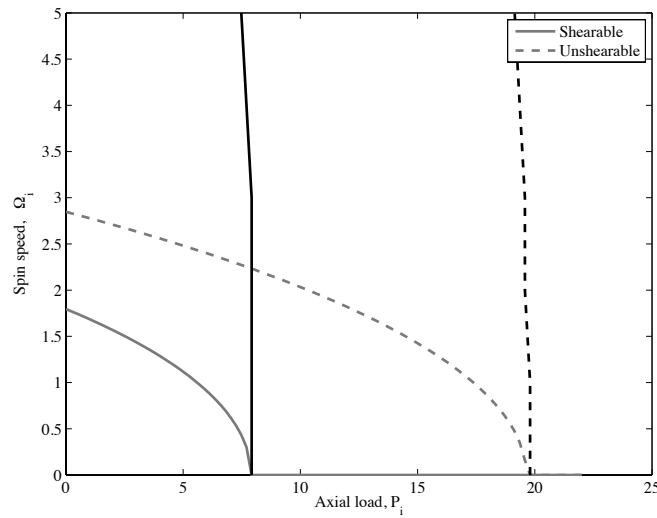


Figure 5: Divergence and flutter instability boundaries in P- Ω plane for $\theta=60^\circ$

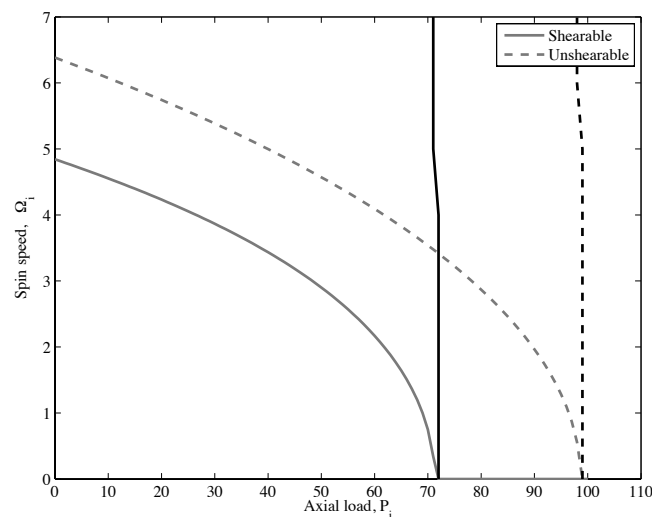


Figure 6: Divergence and flutter instability boundaries in P- Ω plane for $\theta=90^\circ$

CONCLUSION

We have presented the results of dynamic stability analysis of thin-walled composite spinning beam model. Boundaries of divergence and flutter instabilities are established for a wide range of parameters. The major conclusions drawn from this study are listed with no particular order as below:

- In the presence of axial load and for nonzero spin speed we observe that the critical axial loads profoundly increase as the ply angle increases. Besides, the effect of spin speed rate on the critical divergence axial load diminishes for higher ply angles.
- In the presence of axial load and for nonzero spin speed we have also seen that stability regions of both regarding flutter and divergence instabilities expand with the increase of ply angle.

- Lastly, we have reported that the transverse shear has a profound effect in all of the findings listed above and has to be addressed carefully in order to accurately determine the dynamical instabilities of the beams.

Table 2: The boundaries of divergence and flutter instabilities for selected spin speeds and ply-angles

0°				
Ω	Shearable		Unshearable	
	P_{div}	$P_{flutter}$	P_{div}	$P_{flutter}$
0	2.47(2.444[*])	-	2.47	-
1	-	2.44(2.421[*])	-	2.47
2	-	2.37(2.353[*])	-	2.40
3	-	2.24(2.238[*])	-	2.27
4	-	2.08(2.078[*])	-	2.10
5	-	1.88(1.872[*])	-	1.88
45°				
Ω	Shearable		Unshearable	
	P_{div}	$P_{flutter}$	P_{div}	$P_{flutter}$
0	4.08(4.056[*])	-	5.64	-
1	1.75(1.713[*])	4.05(4.033[*])	3.30	5.64
2	-	4.02(3.965[*])	-	5.52
3	-	3.90(3.852[*])	-	5.40
4	-	3.72(3.692[*])	-	5.28
5	-	3.48(3.488[*])	-	5.04
90°				
Ω	Shearable		Unshearable	
	P_{div}	$P_{flutter}$	P_{div}	$P_{flutter}$
0	72.00(71.44[*])	-	99.00	-
1	69.00(69.19[*])	72.00(71.43[*])	96.00	99.00
2	62.00(62.02[*])	72.00(71.39[*])	90.00	99.00
3	48.50(48.61[*])	72.00(71.33[*])	78.00	99.00
4	27.00(26.90[*])	72.00(71.34[*])	62.00	99.00
5	-	71.00(71.13[*])	41.00	99.00

References

- Abbas, L.K., Minjiao, L.I. and Xiaoting, R. (2013) *Transfer matrix method for the determination of the natural vibration characteristics of realistic thrusting launch vehicle-Part I*, Mathematical Problems in Engineering 2013, pp. 1-16.
- Beal, T.R. (1995) *Dynamic stability of a flexible missile under constant and pulsating thrusts*, AIAA Journal 3, pp. 486-494.
- Eken, S. and Kaya, M.O. (2015) *Flexural-torsional coupled vibration of anisotropic thin-walled beams with biconvex cross-section*, Thin-Walled Structures 94, pp. 372-383.
- Librescu, L. and Song, O. (2006) *Thin-walled composite beams: Theory and Application*, The Netherlands: Springer.
- Meitrovich, L. (1997) *Principles and Techniques of Vibrations*, Prentice-Hall.

- Park, Y.P. and Mote, C.D.Jr. (1985) *The maximum controlled follower force on a free-free beam carrying a concentrated mass*, Journal of Sound and Vibration 98, pp. 247-256.
- Park, Y.P. (1987) *Dynamic stability of a free Timoshenko beam under a controlled follower force*, Journal of Sound and Vibration 113, pp. 407-415.
- Platus, D.H., (1992) *Aeroelastic stability of slender, spinning missiles*, Journal of Guidance 15, pp. 144-151.
- Qin, Z. and Librescu, L. (2002) *On a shear-deformable theory of anisotropic thin-walled beams: further contribution and validations*, Composite Structures 56 (4), pp. 345-358.
- Song, O., Jeong N.H. and Librescu, L. (2000) *Vibration and stability of pretwisted spinning thin-walled composite beams featuring bending-bending elastic coupling*, Journal of Sound and Vibration 237 (3), pp. 513-533.
- Song, O., Jeong, N.H. and Librescu, L., (2001) *Implication of conservative and gyroscopic forces on vibration and stability of an elastically tailored rotating shaft modeled as a composite thin-walled beam*, Journal of Acoustical Society of America 109, pp. 972-981.
- Song, O., Librescu, L. and Jeong N.H. (2002) *Vibration and stability control of smart composite rotating shaft via structural tailoring and piezoelectric strain actuation*, Journal of Sound and Vibration 257 (3), pp. 503-525.
- Sugiyama, Y., Katayama, K., and Kinoi, S. (1995) *Flutter of cantilevered column under rocket thrust*, Journal of Aerospace Engineering 8, pp. 9-15.
- Sugiyama, Y., Matsuike, J., Ryu, J.B., Katayama, K., Kinoi, S., and Enomoto, N., (1995) *Effect of Concentrated Mass on Stability of Cantilevers Under Rocket Thrust*, AIAA Journal 33, pp. 499-503.
- Yoon, S.J. and Kim, J.H. (2002) *A concentrated mass on the spinning unconstrained beam subjected to a thrust*, Journal of Sound and Vibration 254, pp. 621-634.